SUPRAMOLECULAR COCRYSTALS: SYNTHESIS, STRUCTURAL CHARACTERIZATIONS AND THEORETICAL STUDIES

NURIDAYANTI BINTI CHE KHALIB

UNIVERSITI SAINS MALAYSIA
2017

SUPRAMOLECULAR COCRYSTALS: SYNTHESIS, STRUCTURAL CHARACTERIZATIONS AND THEORETICAL STUDIES

by

NURIDAYANTI BINTI CHE KHALIB

Thesis submitted in fulfillment of the requirements for the degree of Doctor of Philosophy

June 2017

ACKNOWLEDGEMENT

بِسْمِ اللهِ الرَّحْمٰنِ الرَّحِيْمِ

Greatest thanks to my supervisor, Prof. Dr. Abdul Razak Ibrahim. I really appreciate all the support, guidance and encouragement as well as his patience and empathetic nature. You are a great supervisor indeed.

I also thank my co-supervisor, Dr. Suhana Arshad for her effort, valuable suggestions and for sharing her expertise in guiding me through my journey. Also not forgetting Dr. Kaliyaperumal Thanigaimani who has assisted and taught me in during my PhD research.

I would like to take this opportunity to thank the Malaysian government for awarding me MyBrain15 (MyPhD) scholarship and Universiti Sains Malaysia for USM Short Term Grant (No. 304/PFIZIK/6312078) to fund this PhD research.

My gratitude to Dr. Loh Wan Sin, Mr. Chia Tze Shang, Mr. Mustaqim Rosli, Mr. Noor Aswafi, Mr. Mustaqim Abu Bakar, Mr. Kwong Huey Chong, Mrs Dian Alwani Zainuri and Miss Li Yee from the Crystallography Laboratory, School of Physics, for the invaluable help and advice along the way. Thank you so much to everyone for keeping me smiling, laughing and motivated when I was feeling down especially Dr. Suhana Arshad. You are all the best friends I ever had.

I am grateful to my family, especially my husband, Mr. Kamaruddin Mat Ali @ Hamad for his support and for always brightening my day throughout my PhD research journey. Thanks to my mum, Mrs. Jamenah Awang, siblings and in-laws for supporting and encouraging me unceasingly. This thesis is specially dedicated to my dad, Mr. Che Khalib Hamid. Miss you a lot ‘ABAH’.

TABLE OF CONTENTS

ACKNOWLEDGEMENT ii

TABLE OF CONTENTS iii

LIST OF TABLES viii

LIST OF FIGURES xi

LIST OF PLATES xix

LIST OF SCHEMES xx

LIST OF ABBREVIATIONS xxi

ABSTRAK xxiii

ABSTRACT xxiv

CHAPTER 1 – INTRODUCTION 1

1.1 Supramolecular Chemistry 1

1.2 Crystal Engineering 2

1.3 Hydrogen Bonding 3

1.3.1 Graph-sets of hydrogen bonded motifs 3

1.3.2 Supramolecular Synthons 5

1.4 Cocrystals 8

1.5 Problem Statement 10

1.6 Scope of the Research Work 10

1.7 Objectives 11

CHAPTER 2 – LITERATURE REVIEW 12

2.1 Nitrogen Heterocyclic Compound 13

2.2 Supramolecular Structure and Characterization of Cocrystal 14

2.3 Spectroscopic Studies 25

CHAPTER 3 – THEORY AND METHODOLOGY 29

3.1 Synthesis and Crystallization of Single Crystals 29

3.1.1 Preparation of 2-amino-5-chloropyridine with *ortho*, *meta* and *para*-methylbenzoic acid and 2-methoxybenzoic acid [1 (a–d)], Preparation 2-amino-4-chloropyridine with 2-aminobenzoic acid [1e] 29

3.1.2 Preparation of 2-amino-5-bromopyridine with *ortho*, *meta* and *para*-methylbenzoic acid [2 (a–c)], Preparation of 2-amino-3-bromopyridine with 4-methylbenzoic acid [2d] 30

3.1.3 Preparation of 2-amino-5-nitropyridine with *para*-methylbenzoic acid (3a) and *meta*-chlorobenzoic acid (3b) 30

3.1.4 Preparation of 2, 6-diamino-4-chloropyrimidine with benzoic acid (4) 30

3.1.5 Preparation of 2-amino-4-chloro-6-methoxypyrimidine with *para*- methylbenzoic acid (5a) and succinic acid (5b) 30

3.1.6 Preparation of 2-amino-4-chloro-6-methylpyrimidine with *para*- methylbenzoic acid (6a) and 3-chlorobenzoic acid (6b) 30

3.1.7 Preparation of 2, 4-diamino-6-(4-methylphenyl)-1, 3, 5-triazine with benzoic acid, *meta* and *para*-methylbenzoic acid [7 (a-c)] 31

3.2 Single Crystal X-ray Crystallography 31

3.2.1 Sample Preparation and Data Processing 32

3.3 Powder Crystal X-ray Crystallography 37

3.3.1 Sample Preparation for Powder X-Ray Diffractometer (PXRD) 38

3.4 Fourier Transform Infra-Red (FT-IR) Spectroscopy 40

3.4.1 Sample Preparation for FT-IR Spectroscopy 42

3.5 Nuclear Magnetic Resonance (NMR) Spectroscopy 43

3.5.1 Sample Preparation for NMR Spectroscopy 44

3.6 Density Functional Theory (DFT) Study 45

3.7 Hirshfeld Surface Study 46

CHAPTER 4 – RESULTS AND DISCUSSION 50

4.1 Introduction 50

4.2 Prediction of pKa Values 51

4.3 NMR Studies 52

4.4 Powder XRD Studies 54

4.5 Single Crystal XRD Studies 60

4.5.1 2-amino-5-chloropyridine with 2-, 3-, 4-methylbenzoic acid, 2-methoxybenzoic acid 1 (a-d), 2-amino-4-chloropyridine with 2-aminobenzoic acid (1e) 60

4.5.1(a) X-Ray Crystal Structures 63

4.5.1(b) Geometry Optimization 71

4.5.1(c) Supramolecular Structures 72

4.5.1(d) Hirshfeld Surfaces Analysis with Fingerprint Plots 77

4.5.2 2-amino-5-bromopyridine with 2-, 3-, 4-methylbenzoic acid, 2 (a-c), 2-amino-3-bromopyridine with 4-methylbenzoic acid (2d) 84

4.5.2(a) X-Ray Crystal Structures 87

4.5.2(b) Geometry Optimization 89

4.5.2(c) Supramolecular Structures 94

4.5.2(d) Hirshfeld Surfaces Analysis with Fingerprint Plots 98

4.5.3 2-amino-5-nitropyridine with 4-methylbenzoic acid (3a) and 3-chlorobenzoic acid (3b) 104

4.5.3(a) X-Ray Crystal Structures 106

4.5.3(b) Geometry Optimization 107

4.5.3(c) Supramolecular Structures 110

4.5.3(d) Hirshfeld Surfaces Analysis with Fingerprint Plot 113

4.5.4 2, 6-diamino-4-chloropyrimidine with Benzoic acid (4) 118

4.5.4(a) X-Ray Crystal Structure 120

4.5.4(b) Geometry Optimization 121

4.5.4(c) Supramolecular Structure 123

4.5.4(d) Hirshfeld Surfaces Analysis with Fingerprint Plots 124

4.5.5 2-amino-4-chloro-6-methoxypyrimidine with 4-methylbenzoic acid (5a) and Succinic acid (5b) 128

4.5.5(a) X-Ray Crystal Structures 130

4.5.5(b) Geometry Optimization 131

4.5.5(c) Supramolecular Structures 134

4.5.5(d) Hirshfeld Surfaces Analysis with Fingerprint Plots 136

4.5.6 2-amino-4-chloro-6-methylpyrimidine with 4-methylbenzoic acid (6a) and 3-chlorobenzoic acid (6b) 140

4.5.6(a) X-Ray Crystal Structures 142

4.5.6(b) Geometry Optimization 143

4.5.6(c) Supramolecular Structures 146

4.5.6(d) Hirshfeld Surfaces Analysis with Fingerprint Plots 149

4.5.7 2, 4-diamino-6-(4-methylphenyl) – 1, 3, 5-triazine with benzoic acid (7a), 3-methylbenzoic acid (7b) and 4-methylbenzoic acid (7c) 155

4.5.7(a) X-Ray Crystal Structures 157

4.5.7(b) Geometry Optimization 162

4.5.7(c) Supramolecular Structures 163

4.5.7(d) Hirshfeld Surfaces Analysis with Fingerprint Plots 167

4.6 Vibrational Analysis 172

4.6.1 Vibrational Analysis for 1 (a–e) 172

4.6.2 Vibrational Analysis for 2 (a–d) 178

4.6.3 Vibrational Analysis for 3a and 3b 182

4.6.4 Vibrational Analysis for 4 185

4.6.5 Vibrational Analysis for 5a and 5b 187

4.6.6 Vibrational Analysis for 6a and 6b 190

4.6.7 Vibrational Analysis for 7 (a–c) 193

CHAPTER 5 – CONCLUSION AND RECOMMENDATION 198

5.1 Conclusion 198

5.2 Recommendation 200

REFERENCES 201

APPENDICES

THESIS-RELATED PUBLICATIONS

LIST OF PUBLICATIONS

LIST OF TABLES

		Page
Table 4.1	List of cocrystals	50
Table 4.2	pKa values of the components involved in cocrystal formation	51
Table 4.3	The ^{1}H NMR values of cocrystals.	52
Table 4.4a	Crystallographic informations of 1 (a–c).	61
Table 4.4b	Crystallographic informations of 1d and 1e.	62
Table 4.5	Hydrogen bonding geometry (Å, °) for 1 (a–e).	63
Table 4.6a	Selected experimental and optimized geometrical parameters of 1a.	66
Table 4.6b	Selected experimental and optimized geometrical parameters of 1b.	67
Table 4.6c	Selected experimental and optimized geometrical parameters of 1c.	68
Table 4.6d	Selected experimental and optimized geometrical parameters of 1d.	69
Table 4.6e	Selected experimental and optimized geometrical parameters of 1e.	70
Table 4.7a	Crystallographic informations of 2a and 2b.	85
Table 4.7b	Crystallographic informations of 2c and 2d.	86
Table 4.8	Hydrogen bonding geometry (Å, °) for 2 (a–d).	87
Table 4.9a	Selected experimental and optimized geometrical parameters of 2a.	90
Table 4.9b	Selected experimental and optimized geometrical parameters of 2b.	91
Table 4.9c	Selected experimental and optimized geometrical parameters of 2c.	92
Table 4.9d	Selected experimental and optimized geometrical parameters of 2d.	93

Table 4.10	Crystallographic informations of 3a and 3b.	105
Table 4.11	Hydrogen bonding geometry (Å, °) for 3a and 3b.	106
Table 4.12a	Selected experimental and optimized geometrical parameters of 3a.	108
Table 4.12b	Selected experimental and optimized geometrical parameters of 3b.	109
Table 4.13	Crystallographic informations of 4.	119
Table 4.14	Hydrogen bonding geometry (Å, °) for 4.	120
Table 4.15	Selected experimental and optimized geometrical parameters of 4.	122
Table 4.16	Crystallographic informations of 5a and 5b.	129
Table 4.17	Hydrogen bonding geometry (Å, °) for 5a and 5b.	130
Table 4.18a	Selected experimental and optimized geometrical parameters of 5a.	132
Table 4.18b	Selected experimental and optimized geometrical parameters of 5b.	133
Table 4.19	Crystallographic informations of 6a and 6b.	141
Table 4.20	Hydrogen bonding geometry (Å, °) for 6a and 6b.	142
Table 4.21a	Selected experimental and optimized geometrical parameters of 6a.	144
Table 4.21b	Selected experimental and optimized geometrical parameters of 6b.	145
Table 4.22	Crystallographic informations of 7 (a–c).	156
Table 4.23	Hydrogen bonding geometry (Å, °) for 7 (a–c).	157
Table 4.24a	Selected experimental and optimized geometrical parameters of 7a.	159
Table 4.24b	Selected experimental and optimized geometrical parameters of 7b.	160
Table 4.24c	Selected experimental and optimized geometrical parameters of 7c.	161

Table 4.25	The experimental and calculated vibrational frequency of 1 (a–e).	176
Table 4.26	The experimental and calculated vibrational frequency of 2 (a–d).	181
Table 4.27	The experimental and calculated vibrational frequency of 3a and 3b.	184
Table 4.28	The experimental and calculated vibrational frequency of 4.	186
Table 4.29	The experimental and calculated vibrational frequency of 5a and 5b.	189
Table 4.30	The experimental and calculated vibrational frequency of 6a and 6b.	192
Table 4.31	The experimental and calculated vibrational frequency of 7 (a–c).	196

LIST OF FIGURES

		Page
Figure 1.1	The most common supramolecular synthons.	5
Figure 1.2	Supramolecular heterosynthons (a) $R_2^2(7)$ acid-base heterodimer synthon (b) The carboxylic acid–amide supramolecular heterosynthon in the tetrameric motif and (c) The heterodimer, $R_2^2(7)$ and expanded ring $R_4^4(24)$.	7
Figure 1.3	Schematic of cocrystals.	9
Figure 2.1	Examples of cocrystals and salts.	15
Figure 2.2	(a) Scheme and (b) the crystal packing of the molecular structure of 2-amino-5-chloropyridine benzoic acid.	16
Figure 2.3	(a) Scheme and (b) the crystal packing of the molecular structure of 2-amino-5-bromopyridine benzoic acid.	17
Figure 2.4	Molecular structure of 2-amino-4,6-dimethoxypyrimidine 4-aminobenzoic acid: (a) Hydrogen bond pattern and (b) hydrogen pattern in supramolecular chain along the *c*-axis.	18
Figure 2.5	Hydrogen pattern in 2-amino-6-chloropyridine represent homosynthon.	18
Figure 2.6	Hydrogen pattern in 2-amino-6-chloropyridine benzoic acid represent (a) $R_2^2(8)$ ring motif heterosynthon; (b) supramolecular zig-zag chains.	19
Figure 2.7	View of the complementary DADA arrays of quadruple hydrogen pattern in 2-amino-6-chloropyridine 3-chloropyridine.	20
Figure 2.8	View of heterotetramer infinite tape connected by $R_2^2(6)$ synthon.	28
Figure 2.9	Supramolecular sheet formed by interconnection of tape along (122) plane.	29
Figure 2.10	View of extension infinite tape connected by $R_2^2(6)$ synthon.	22

Figure 2.11	(a) The asymmetric unit and (b) the crystal packing of 2,4-diamino-6-phenyl-1,3,5-triazine–sorbic acid (1/1) showing 50% probability displacement ellipsoids. Dashed lines indicate hydrogen bonds [symmetry code: (i) x, $-y+1$, $z-1/2$; (ii) x, $-y$, $z-1/2$; (iii) x, $-y$, $z+1/2$].	23
Figure 2.12	(a) Linear acid formed 8-membered cyclic tape network; (b) Bent acid formed 6-membered cyclic tape network.	24
Figure 2.13	(a) The transoid geometry and (b) the cisoid geometry of the carboxylic acids in cocrystals of 2, 4-diamino-6-phenyl- 1, 3, 5-triazine.	24
Figure 2.14	IR spectrum of for 2-amino-6-chloropyridine benzoic acid.	25
Figure 2.15	FT-IR spectrum of 2, 4-diamino-6-phenyl-1, 3, 5-triazine with various carboxylic acids.	26
Figure 2.16	^{1}H and ^{13}C NMR spectrum of for 2-amino-6-chloropyridine benzoic acid.	27
Figure 2.17	Powder XRD pattern of 2-amino-6-chloropyridine benzoic acid.	27
Figure 2.18	PXRD patterns of the cocrystals and the individual components under various conditions.	28
Figure 3.1	Plot of 2θ *vs* X-ray intensity.	39
Figure 3.2	An example of IR absorption region.	40
Figure 3.3	The types of vibrations in molecular structure.	41
Figure 3.4	The example of IR spectrum plotted in percent transmittance (%T).	41
Figure 3.5	The NMR signal with TMS at the end of the spectrum.	43
Figure 3.6	The Hirshfeld surface of the molecule is shown in transparent mode, and the distances d_i and d_e illustrated schematically for a single point (red dot).	48
Figure 3.7	2-chloro-4-nitrobenzoic acid: (a) Hirshfeld surface mapped on d_{norm} with the neighboring molecules and (b) Fingerprint plots with the intermolecular contact is circled in red.	48
Figure 3.8	Front and back views of the Hirshfeld surface of 2-chloro-4-nitrobenzoic acid, mapped with the shape index and curvedness.	49

Figure 4.1	The PXRD pattern for 1 (a–e).	55
Figure 4.2	The PXRD pattern for 2 (a–d).	56
Figure 4.3	The PXRD pattern for 3a and 3b.	57
Figure 4.4	The PXRD pattern for 4.	57
Figure 4.5	The PXRD pattern for 5a and 5b.	58
Figure 4.6	The PXRD pattern for 6a and 6b.	58
Figure 4.7	The PXRD pattern for 7 (a–c).	59
Figure 4.8	The molecular and optimized structures of 1 (a–e).	65
Figure 4.9	Hydrogen bonding interactions in 1a: (a) supramolecular heterosynthons forming a zig-zag chain; (b) C—H···π interactions.	73
Figure 4.10	Hydrogen bonding interactions in 1b: (a) supramolecular heterosynthons forming helical chain; (b) supramolecular 2-dimensional *ab* plane formed *via* C—H···O interaction.	74
Figure 4.11	Hydrogen bonding interactions in 1c: (a) supramolecular heterosynthons forming a chain; (b) π···π interactions.	75
Figure 4.12	Hydrogen bonding interactions in 1d forming $R_2^2(8)$ and $R_1^2(6)$ ring motif.	76
Figure 4.13	The DADA array of hydrogen bonding motif with graph-set notation of $R_2^2(8), R_4^2(8)$ and $R_2^2(8)$ in 1e.	77
Figure 4.14	d_{norm} mapped on Hirshfeld surfaces for visualizing the intermolecular interactions of the 1a with fingerprint plot percentage contributions. Dotted lines (green) represent hydrogen bonds.	78
Figure 4.15	d_{norm} mapped on Hirshfeld surfaces for visualizing the intermolecular interactions of the 1b with fingerprint plot percentage contributions. Dotted lines (green) represent hydrogen bonds.	79
Figure 4.16	d_{norm} mapped on Hirshfeld surfaces for visualizing the intermolecular interactions of the 1c with fingerprint plot percentage contributions. Dotted lines (green) represent hydrogen bonds.	80

Figure 4.17	Hirshfeld surfaces mapped over (a) the shape index and (b) the curvedness in 1c.	81
Figure 4.18	d_{norm} mapped on Hirshfeld surfaces for visualizing the intermolecular interactions of the 1d with fingerprint plot percentage contributions. Dotted lines (green) represent hydrogen bonds.	82
Figure 4.19	d_{norm} mapped on Hirshfeld surfaces for visualizing the intermolecular interactions of the 1e with fingerprint plot percentage contributions. Dotted lines (green) represent hydrogen bonds.	83
Figure 4.20	The molecular and optimized structures of 2 (a–d).	88
Figure 4.21	The packing diagram of 2a.	95
Figure 4.22	The packing diagram of 2b.	95
Figure 4.23	The packing diagram of 2c: (a) supramolecular chain along *c*-axis; (b) a layer parallel to the *bc*-plane and (c) C—H···π interactions.	96
Figure 4.24	The packing diagram of 2d: (a) supramolecular chain down *b*-axis; (b) supramolecular chains interconnected by weak C—H···π and π–π interactions.	97
Figure 4.25	d_{norm} mapped on Hirshfeld surfaces for visualizing the intermolecular interactions of the 2a with fingerprint plot percentage contributions. Dotted lines (green) represent hydrogen bonds.	98
Figure 4.26	d_{norm} mapped on Hirshfeld surfaces for visualizing the intermolecular interactions of the 2b with fingerprint plot percentage contributions. Dotted lines (green) represent hydrogen bonds.	99
Figure 4.27	d_{norm} mapped on Hirshfeld surfaces for visualizing the intermolecular interactions of the 2c with fingerprint plot percentage contributions. Dotted lines (green) represent hydrogen bonds.	100
Figure 4.28	d_{norm} mapped on Hirshfeld surfaces for visualizing the intermolecular interactions of the 2d with fingerprint plot percentage contributions. Dotted lines (green) represent hydrogen bonds**.**	102
Figure 4.29	Hirshfeld surfaces mapped over the shape index of 2d (a) front view and (b) back view.	103

Figure 4.30	Hirshfeld surfaces mapped over the curvedness of 2d (a) front view and (b) back view.	103
Figure 4.31	The molecular and optimized structures of 3a and 3b.	106
Figure 4.32	The packing pattern of 3a: (a) the graph–set notations $R_2^2(8), R_4^2(8)$ and $R_2^2(8)$ arrangement and (b) weak π—π interactions.	111
Figure 4.33	The packing diagram of 3b.	112
Figure 4.34	d_{norm} mapped on Hirshfeld surfaces for visualizing the intermolecular interactions of the 3a with fingerprint plot percentage contributions. Dotted lines (green) represent hydrogen bonds.	114
Figure 4.35	Hirshfeld surfaces mapped over (a) the shape index and (b) the curvedness in 3a.	115
Figure 4.36	d_{norm} mapped on Hirshfeld surfaces for visualizing the intermolecular interactions of the 3b with fingerprint plot percentage contributions. Dotted lines (green) represent hydrogen bonds.	116
Figure 4.37	Hirshfeld surfaces mapped over (a) the shape index and (b) the curvedness in 3b.	117
Figure 4.38	The molecular and optimized structures of 4.	120
Figure 4.39	(a) The packing diagram of 4; (b) C—H···π interactions of 4.	124
Figure 4.40	d_{norm} mapped on Hirshfeld surfaces for visualizing the intermolecular interactions of the 4 with fingerprint plot percentage contributions. Dotted lines (green) represent hydrogen bonds.	126
Figure 4.41	Hirshfeld surfaces mapped over (a) the shape index and (b) the curvedness in 4.	127
Figure 4.42	The molecular and optimized structures of 5a and 5b.	130
Figure 4.43	The packing pattern of 5a.	135
Figure 4.44	The packing pattern of 5b.	136
Figure 4.45	d_{norm} mapped on Hirshfeld surfaces for visualizing the intermolecular interactions of the 5a with fingerprint plot percentage contributions. Dotted lines (green) represent hydrogen bonds.	137

Figure 4.46	Hirshfeld surfaces mapped over the shape index and the curvedness of 5a.	138
Figure 4.47	d_{norm} mapped on Hirshfeld surfaces for visualizing the intermolecular interactions of the 5b with fingerprint plot percentage contributions. Dotted lines (green) represent hydrogen bonds.	139
Figure 4.48	The molecular and optimized structures of 6a and 6b.	142
Figure 4.49	The packing pattern of 6a: (a) heterotetrameric synthon, (b) π-π stacking interactions.	147
Figure 4.50	The packing pattern of 6b.	149
Figure 4.51	d_{norm} mapped on Hirshfeld surfaces for visualizing the intermolecular interactions of the 6a with fingerprint plot percentage contributions. Dotted lines (green) represent hydrogen bonds.	151
Figure 4.52	Hirshfeld surfaces mapped over (a) the shape index and (b) the curvedness of 6a.	151
Figure 4.53	d_{norm} mapped on Hirshfeld surfaces for visualizing the intermolecular interactions of the 6b with fingerprint plot percentage contributions. Dotted lines (green) represent hydrogen bonds.	152
Figure 4.54	Hirshfeld surfaces mapped over (a) the shape index and (b) the curvedness of 6b.	154
Figure 4.55	The molecular and optimized structures of 7 (a–c).	158
Figure 4.56	The packing diagram of 7a: (a) supramolecular ribbon and (b) C—H···π interactions.	164
Figure 4.57	The packing diagram of 7b: (a) supramolecular ribbon and (b) C—H···π interactions.	165
Figure 4.58	The packing diagram of 7c: (a) supramolecular ribbon and (b) C—H···π interactions.	166
Figure 4.59	d_{norm} mapped on Hirshfeld surfaces for visualizing the intermolecular interactions of the 7a with fingerprint plot percentage contributions. Dotted lines (green) represent hydrogen bonds.	168
Figure 4.60	Hirshfeld surfaces mapped over (a) the shape index and (b) the curvedness in 7a (Front view).	169

Figure 4.61	Hirshfeld surfaces mapped over (a) the shape index and (b) the curvedness in 7a (Back view).	169
Figure 4.62	d_{norm} mapped on Hirshfeld surfaces for visualizing the intermolecular interactions of the 7b with fingerprint plot percentage contributions. Dotted lines (green) represent hydrogen bonds.	170
Figure 4.63	d_{norm} mapped on Hirshfeld surfaces for visualizing the intermolecular interactions of the 7c with fingerprint plot percentage contributions. Dotted lines (green) represent hydrogen bonds.	171
Figure 4.64a	The theoretical and experimental IR spectrum for 1a in comparison with the parent compounds (2MBA and 2A5CP).	173
Figure 4.64b	The theoretical and experimental IR spectrum for 1b in comparison with the parent compounds (3MBA and 2A5CP).	173
Figure 4.64c	The theoretical and experimental IR spectrum for 1c in comparison with the parent compounds (4MBA and 2A5CP).	174
Figure 4.64d	The theoretical and experimental IR spectrum for 1d in comparison with the parent compounds (2MOBA and 2A5CP).	174
Figure 4.64e	The theoretical and experimental IR spectrum for 1e in comparison with the parent compounds (2ABA and 2A4CP).	175
Figure 4.65a	The theoretical and experimental IR spectrum for 2a in comparison with the parent compounds (2MBA and 2A5BP).	178
Figure 4.65b	The theoretical and experimental IR spectrum for 2b in comparison with the parent compounds (3MBA and 2A5BP).	179
Figure 4.65c	The theoretical and experimental IR spectrum for 2c in comparison with the parent compounds (4MBA and 2A5BP).	179
Figure 4.65d	The theoretical and experimental IR spectrum for 2d in comparison with the parent compounds (4MBA and 2A3BP).	180
Figure 4.66a	The theoretical and experimental IR spectrum for 3a in comparison with the parent compounds (4MBA and 2A5NP).	183
Figure 4.66b	The theoretical and experimental IR spectrum for 3b in comparison with the parent compounds (3CBA and 2A5NP).	183
Figure 4.67	The theoretical and experimental IR spectrum for 4 in comparison with the parent compounds (BA and DCPY).	186

Figure 4.68a	The theoretical and experimental IR spectrum for 5a in comparison with the parent compounds (4MBA and 2CMOP).	188
Figure 4.68b	The theoretical and experimental IR spectrum for 5b in comparison with the parent compounds (Succinic acid and 2CMOP).	188
Figure 4.69a	The theoretical and experimental IR spectrum for 6a in comparison with the parent compounds (4MBA and 2CMEP).	191
Figure 4.69b	The theoretical and experimental IR spectrum for 6b in comparison with the parent compounds (3CBA and 2CMEP).	191
Figure 4.70a	The theoretical and experimental IR spectrum for 7a in comparison with the parent compounds (BA and 2DMPT).	194
Figure 4.70b	The theoretical and experimental IR spectrum for 7b in comparison with the parent compounds (3MBA and 2DMPT).	194
Figure 4.70c	The theoretical and experimental IR spectrum for 7c in comparison with the parent compounds (4MBA and 2DMPT).	195

LIST OF PLATES

		Page
Plate 3.1	(a) Crystal attached to a fine glass fiber with super glue; (b) Rotation photo for a good single crystal.	32
Plate 3.2	(a) SMART APEX II system; (b) Bruker SMART APEX II DUO system.	33
Plate 3.3	Preparation of sample for XRD.	38
Plate 3.4	Bruker D8 Advance diffractometer.	39
Plate 3.5	Perkin Elmer Spotlight 200 Spectrometer.	42
Plate 3.6	Preparation of sample for NMR analysis.	44
Plate 3.7	Bruker AVANCE III 500 MHz Spectrometer.	45

LIST OF SCHEMES

		Page
Scheme 1.1	Examples of graph-set notations in hydrogen-bonded motifs.	4
Scheme 2.1	The schematic of nitrogen heterocyclic such as pyridine, pyrimidine and triazine.	13
Scheme 4.1	The schematic diagram of 1 (a–e).	60
Scheme 4.2	The schematic diagram of 2 (a–d).	84
Scheme 4.3	The schematic diagram of 3a and 3b.	104
Scheme 4.4	The schematic diagram of 4.	118
Scheme 4.5	The schematic diagram of 5a and 5b.	128
Scheme 4.6	The schematic diagram of 6a and 6b.	140
Scheme 4.7	The schematic diagram of 7 (a–c).	155

LIST OF ABBREVIATIONS

2ABA	2-aminobenzoic acid
2A3BP	2-amino-3-bromopyridine
2A5BP	2-amino-5-bromopyridine
2A4CP	2-amino-4-chloropyridine
2A5CP	2-amino-5-chloropyridine
2A5NP	2-amino-5-nitropyridine
2CMEP	2-amino-4-chloro-6-methylpyrimidine
2CMOP	2-amino-4-chloro-6-methoxypyrimidine
2DMPT	2, 4-diamino-6-(4-methylphenyl) – 1, 3, 5 – triazine
2MBA	2-methylbenzoic acid
2MOBA	2-methoxybenzoic acid
3CBA	3-chlorobenzoic acid
3MBA	3-methylbenzoic acid
4MBA	4-methylbenzoic acid
BA	Benzoic acid
CSD	Cambridge Structural Database
CCD	Charge-Coupled Device
DADA	Donor-Acceptor-Donor-Acceptor
DCPY	2, 6-diamino-4-chloropyrimidine
DFT	Density Functional Theory
FT-IR	Fourier Transform Infra-Red
IR	Infra-Red

NMR	Nuclear Magnetic Resonance
ppm	parts per million
PXRD	Powder X-Ray Diffraction
SXRD	Single X-Ray Diffraction
SADABS	Siemens Area Detector Absorption Correction
SAINT	SAX Area-detector Integration (SAX-Siemens Analytical X-ray)
SMART	Siemens Molecular Analysis Research Tools
TMS	Tetramethylsilane
wR	Weighted Reliability Index

HABLUR GABUNGAN SUPRAMOLEKUL: SINTESIS, PENCIRIAN STRUKTUR DAN KAJIAN TEORI

ABSTRAK

Dalam kajian ini, sembilan belas hablur gabungan yang baharu dari pelbagai jenis asid karboksilik dan bes telah dikaji menggunakan kaedah spektroskopi seperti Kristalografi sinar-X serbuk dan hablur tunggal, Inframerah (FT-IR) dan Resonan Magnetik Nukleur (NMR). Pengiraan secara teori hablur gabungan telah dilakukan menggunakan kaedah Teori Fungsi Ketumpatan (DFT) dan analisis Permukaan Hirshfeld. Secara umumnya, keputusan DFT dan eksperimen adalah bersesuaian antara satu sama lain kecuali perubahan konformasi di sekeliling kumpulan karbonil. Ciri spektroskopi hablur gabungan telah dikaji menggunakan FT-IR dan NMR. Selain daripada ramalan nilai pKa, pembelauan sinar-X hablur tunggal dan serbuk menunjukkan kesemua sampel adalah hablur gabungan. Struktur molekul dan kehadiran interaksi intermolekul telah disahkan oleh pembelauan sinar-X hablur tunggal dan sumbangan interaksi telah ditunjukan dengan analisis kuantitatif Permukaan Hirshfeld. Pembentukan motif $R_2^2(8)$ heterosinton supramolekul di antara asid karboksilik dan bahagian aminopiridin, aminopirimidin dan aminotriazin boleh dijumpai dalam semua struktur hablur gabungan yang membentuk asas kepada struktur supramolekul. Susunan heterosynthon ini dalam struktur hablur sebahagian dari hablur gabungan telah menghasilkan susunan DADA sinton heterotetramerik kitaran dan sinton heterotetramerik linear. Sinton ini saling bersambungan di dalam struktur hablur semua hablur gabungan melalui pelbagai interaksi intermolekul yang membentuk struktur hablur rantaian, satah 2-dimensi dan rangkaian 3-dimensi.

SUPRAMOLECULAR COCRYSTALS: SYNTHESIS, STRUCTURAL CHARACTERIZATIONS AND THEORETICAL STUDIES

ABSTRACT

In this research work, nineteen novel cocrystals of various carboxylic acids and bases have been investigated using spectroscopic methods such as powder and single crystal X-ray Crystallography, Infrared (FT-IR) and Nuclear Magnetic Resonance (NMR). The theoretical calculations of the cocrystals were performed using Density Functional Theory (DFT) method and Hirshfeld Surfaces analysis. Generally, the DFT and experimental results are comparable to each other except for the conformational difference around the carboxyl groups. Spectroscopic properties of the cocrystals were examined by FT-IR and NMR. Apart from the pKa values prediction, single crystal and powder X-ray diffractions show that all the samples are cocrystals. The molecular structures and the existence of intermolecular interactions have been confirmed by single crystal X-ray diffraction and the contribution of the interactions is shown by quantitative analysis of the Hirshfeld Surfaces. The formation of $R_2^2(8)$ supramolecular heterosynthons motifs between the carboxylic acid and the aminopyridine, aminopyrimidine and aminotriazine moieties can be found in all the cocrystal structures forming the basis of the supramolecular structures. The arrangement of the heterosynthons in the crystal structure of some of the cocrystals generates a DADA array of cyclic heterotetrameric synthon and linear heterotetrameric synthon. These synthons are interconnected within the crystal structure of the cocrystals through various intermolecular interactions forming chains, 2-dimensional planes and 3-dimensional network of crystal structures.

CHAPTER 1

INTRODUCTION

Supramolecular chemistry is generally a study of intermolecular interactions between molecules forming one, two or three – dimensional network. Co-crystallization is a process that unites different molecular species within a single crystalline lattice without involving the formation or breaking of covalent bonds (Gale & Steed, 2012). Cocrystal is a crystalline material that is structurally homogenous with at least two building blocks with definite stoichiometric amounts (Hemamalini *et al.*, 2014).

1.1 Supramolecular Chemistry

Supramolecular chemistry is a highly interdisciplinary field of sciences covering chemical, physical and biological studies of molecular assemblies. Supramolecular chemistry is defined as "*the chemistry of the intermolecular bond, covering the structures and functions of the entities formed by the association of two or more chemical species*" (Lehn, 1995). The most important feature of supramolecular chemistry is the building blocks are reversibly held by intermolecular force that results in non-covalent assembly. The term '*non-covalent*' is related to a vast range of intermolecular interactions that include hydrophobic, electrostatic, hydrogen bond, π-π aromatic and Van der Waals (Lehn, 1995). The non-covalent joining two or more species, termed self-assembly is strictly an equilibrium between two or more molecular components to produce an aggregate with a structure dependent only on the nature of the chemical building blocks (Steed *et al.*, 2007).

1.2 Crystal Engineering

Crystal engineering has been described by a pioneer in the field, as "*the understanding of intermolecular interactions in the context of crystal packing and in the utilization of such understanding in the design of a new solids with desirable physical and chemical properties*" (Desiraju, 1995). Crystal engineering has been approached by mean of understanding of how the molecules interact with other molecules throughout the intermolecular network and then designing a supramolecular strategy to synthesize novel materials with preferred properties and architecture (Moulton & Zaworotko, 2001). The objective of crystal engineering is to design crystal structures by using the molecule as a building block (Desiraju, 2013).

A lot of research in polymorphism (Bernstein, 2002), coordination polymers (Zaworotko, 2001; Mueller *et al.*, 2006), supramolecular synthons (Aakeröy *et al.*, 2001; Aakeröy *et al*., 2002; Bis *et al.*, 2007; Bis & Zaworotko, 2005; Shattock *et al*., 2008; Kavuru *et al.*, 2010; Vishweshar *et al*., 2003), and even pharmaceutical industry (Almarsson & Zaworotko, 2004; Shan & Zaworotko, 2008; Trask *et al.*, 2005; Good & Rodríguez-Hornedo, 2009; Vishweshar *et al.*, 2005) capitalize the crystal engineering concepts.

In crystal engineering features, the identification of proper synthon is very important. Crystal structure of organic compounds is represented as networks of molecules linked by intermolecular interactions. The expectable self-arrangement of molecules into one-, two- or three-dimensional network is of extreme importance in crystal engineering and the structural units forming the network is called supramolecular synthons (Desiraju, 1995).

1.3 Hydrogen Bonding

Hydrogen bonds are highly important in all directional intermolecular interactions in the formation of supramolecular structure. Etter *et al*. (1990) and Bernstein *et al*. (1995) have studied the preferred hydrogen bond arrangement in organic crystals and have suggested the following rules:

- All good proton donors and acceptors are involved in hydrogen bonding.
- Six-membered ring intramolecular hydrogen bonds form in preference to intermolecular hydrogen bonds.
- The best proton donor and acceptor remaining after intramolecular hydrogen bond formation will form intermolecular hydrogen bonds.

1.3.1 Graph-sets of Hydrogen Bonded Motifs

The graph-theory for describing and analyzing hydrogen bond networks in three-dimensional solids was discussed by Etter *et al*. (1990) and Bernstein *et al*. (1995). A generic graph-set descriptor is

$$G_d^a(n) \tag{1.0}$$

Where, G = Graph set designator C, R, D and S

d = Number of donor atoms

a = Number of acceptor atoms

n = Total number of atoms present in the hydrogen bonded motif

The pattern designator has four different assignments which are C, R, D and S based on whether the hydrogen bonds are inter- or intramolecular. C refers to hydrogen-bonded infinite chains, R refers to rings, D refers to non-cyclic dimers. These

designators are used when the graphs set is formed by intermolecular hydrogen bonds. S (self) denotes a ring made of intramolecular hydrogen bonds. The number of donors (d) and acceptor (a) used in each motif are assigned as a subscripts and superscript respectively and the number of atoms (n) involved in the pattern is indicated in the parenthesis. For example, $R_2^2(8)$ graph set notation denotes an eight-membered ring with two hydrogen acceptors and two hydrogen donors, and is exemplified by the carboxylic acid dimer in Scheme 1.1(d).

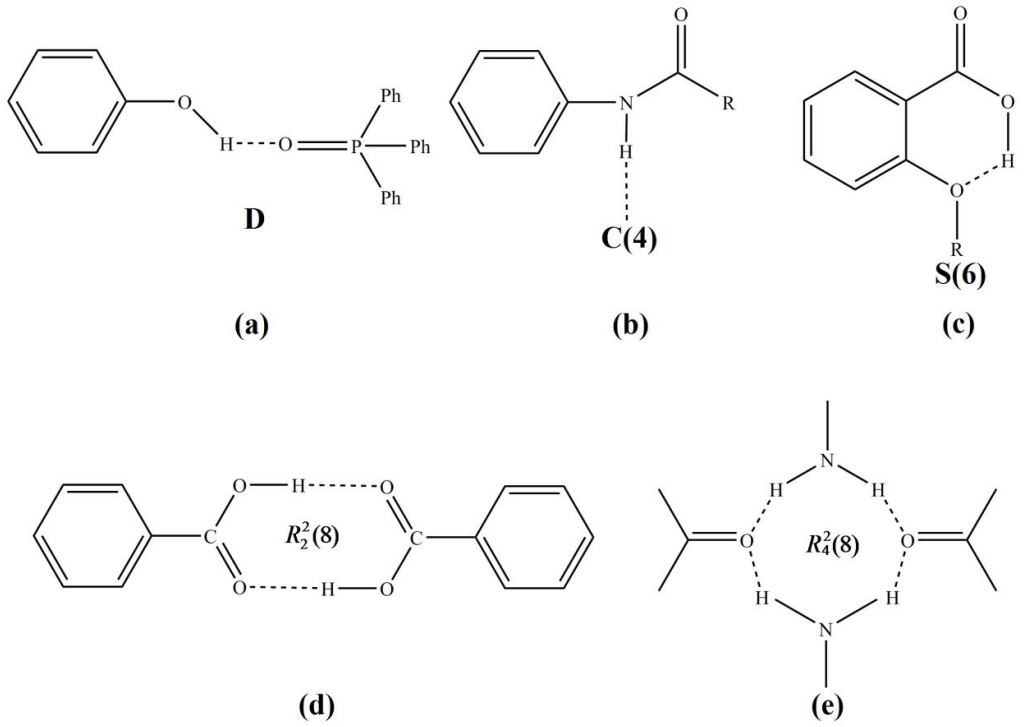

Scheme 1.1 Examples of graph-set notations in hydrogen-bonded motifs (Etter, 1990).

Scheme 1.1 illustrates the examples of graph-set notations in hydrogen-bonded motifs. The use of graph-sets provide an approach in describing the pattern of hydrogen bonded molecules.

1.3.2 Supramolecular Synthons

Supramolecular synthons are intermolecular interactions and hydrogen bond motifs that are formed repetitively in molecular crystal structures (Desiraju, 1995). Supramolecular synthons are divided into two categories which are supramolecular homosynthons and supramolecular heterosynthons.

A supramolecular homosynthon is formed between identical functional groups, for example between two carboxylic acid moieties to form a dimer while a supramolecular heterosynthon is formed between complementary but different functional groups, such as between carboxylic acid and amide moieties (Rodríguez-Spong *et al.*, 2004). Figure 1.1 illustrates the most common supramolecular synthons in crystal engineering.

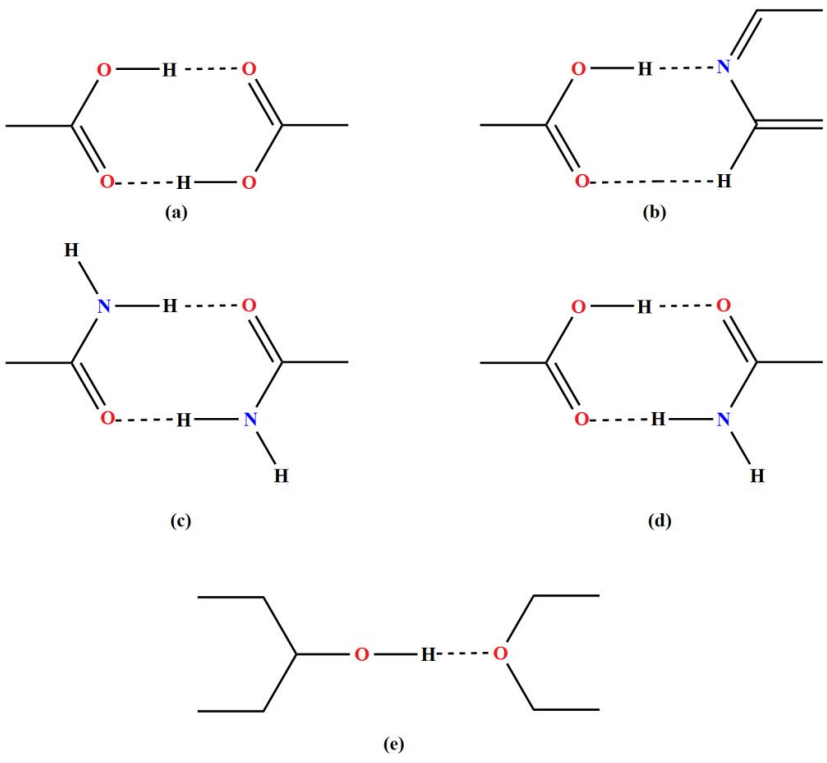

Figure 1.1 The most common supramolecular synthons (Qiao *et al.*, 2011).

The most commonly used supramolecular synthons in crystal engineering are homosynthon formed between carboxylic acid dimer (Figure 1.1a), heterosynthon formed between carboxylic acid and pyridine groups (Figure 1.1b), homosynthon formed between amide dimer (Figure 1.1c), heterosynthon formed between carboxylic acid and amide groups (Figure 1.1d) and heterosynthon formed between alcohol and ether groups (Figure 1.1e) (Qiao *et al.*, 2011).

Supramolecular heterosynthons generally employed the carboxylic acid-aromatic N-heterocyclic due to its strength and reliability (Desiraju, 1995). Cambridge Structural Database (CSD) analysis by Shattock *et al.* (2008), they revealed that the COOH···N_{arom} supramolecular heterosynthon involving carboxylic acids (-COOH) are strongly favoured over supramolecular homosynthons. This thesis are focusing on the ability of carboxylic acid to form reliable supramolecular heterosynthons with N-heterocyclics such as pyridines, pyrimidines and triazines derivatives which are useful in preparing desired multi-component system in material science research.

Several reports have discussed the importance of understanding supramolecular heterosynthons in the synthesis of cocrystals (Trask *et al*., 2005; Vishweswar *et al*., 2005; Fleischman *et al*., 2003; Bettinetti, *et al.*, 2000; Mohamed *et al*., 2009). Figure 1.2 shows the example of supramolecular heterosynthons reported previously.

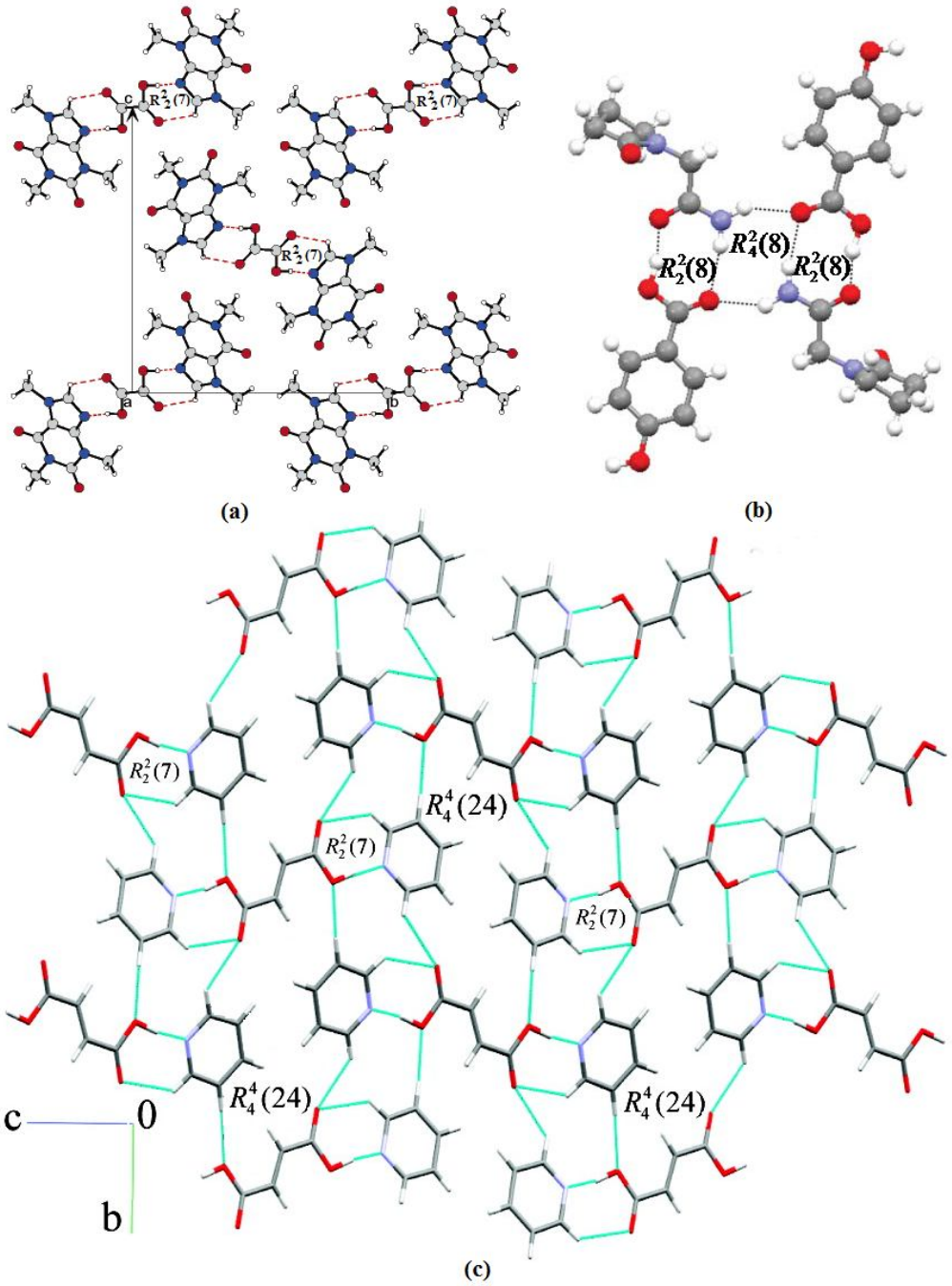

Figure 1.2 Supramolecular heterosynthons (a) $R_2^2(7)$ acid-base heterodimer synthon (Trask *et al.*, 2005), (b) The carboxylic acid–amide supramolecular heterosynthon in the tetrameric motif (Vishweswar *et al.*, 2005) and (c) The heterodimer, $R_2^2(7)$ and expanded ring $R_4^4(24)$ (Mohamed *et al*., 2009).

1.4 Cocrystals

Cocrystal can be defined as a crystalline solid containing multiple components with at least two or more molecules associated through intermolecular interactions (Childs *et al*., 2007). In a supramolecular perspective, the molecules of the crystal are held together by supramolecular synthons. One of these molecules is known as the cocrystal former which forms supramolecular synthons with the other molecules (Shattock *et al*., 2008).

Cocrystal is one of the important themes in supramolecular studies and is gaining interest across a variety of research disciplines. Crystal engineering and supramolecular chemistry have motivated researches on the design of materials by directing molecular assembly of different components in the crystalline state to form cocrystals (Trask *et al.*, 2005). Intermolecular interactions have a significant contribution in the synthesis of cocrystal due to their strength and directional nature. Traditional O—H···O and O—H···N strong hydrogen bonds, weaker C—H···π or C—H···Cl and other molecules association such as halogen-halogen, nitro-nitro and π ···π interactions are normally employed in cocrystal synthesis (Trask & Jones, 2005).

A neutral compound has potential to interact with a cocrystal former in cocrystallization processes as shown in Figure 1.3. Cocrystal former can include organic acids or bases that remain in their neutral form within the multi-component crystal and exists as a solid at ambient conditions (Almarssön & Zaworotko, 2004; Aakeröy *et al*., 2007).

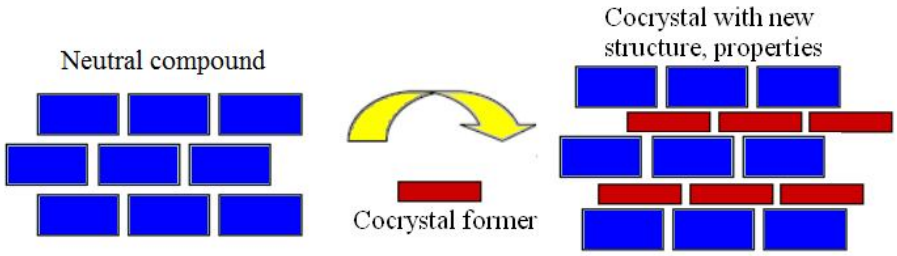

Figure 1.3 Schematic of cocrystals.

Cocrystal is one of a variety of distinct solid forms that display the unique of physicochemical properties which can greatly influence the bioavailability, manufacturabiliy, purification, stability and other performance characteristics of drug (Yadav *et al.*, 2009). Most of cocrystals have been reacted through strong hydrogen bonds, O—H···N which is notable between a carboxylic acid and an N-heterocyclic hydrogen-bond acceptor (Aakeröy *et al*., 2007; Aakeröy *et al*., 2006; Aakeröy *et al*., 2005). However, the reaction between these components can also resulted in a salt formation when the acid is protonated to the base/ ligand (Banerjee *et al*., 2005). The interaction of O—H···N will be replaced with a charge transferred $O^{-}\cdots H—N^{+}$ hydrogen bond (Aakeröy *et al*., 2007). The design of complexes of cocrystals and salts, with are neutral and charged component, respectively are the current avenue of research in solid-state organic chemistry (Lemmerer *et al*., 2015). The design of molecular network based on hydrogen bond has appeared as an impressive mechanism in the discovery of cocrystals (Hornedo, 2007).

1.5 Problem Statement

Cocrystals have attracted a lot of attentions in recent years especially in pharmaceutical industries. These cocrystals are used to improve the physicochemical properties of drugs. Before the physicochemical test can be done, the candidate cocrystals must be identified, synthesized and analyzed for their structural properties. These would consumed extra time before they can be tested for physicochemical improvement. This research would identify cocrystals to be synthesized and analyzed. These cocrystals would provide a pool of candidates for the physicochemical test to analyze the improvement of the physicochemical properties of the drug substance. This would help in rapid testing of the physicochemical properties with the help of readily available candidates to be chosen from.

1.6 Scope of the Research Work

The most widely used synthons for directed assembly of cocrystals involve a carboxylic acid in combination with a suitable N-heterocyclic compound (Shattock *et al.*, 2008). Most of organic molecular cocrystals have been assembled through a strong hydrogen bond, O—H···N that is expected from a carboxylic acid···N (heterocyclic) interaction. This research will be focusing on the synthesis of the supramolecular cocrystals from N-heterocyclic compounds such as pyridine, pyrimidine and triazine with carboxylic acid to form reliable supramolecular heterosynthons that persist in the presence of competing functionalities. The structural behaviour of the compounds will also be analyzed using experimental and theoretical methods. The formation of non-covalent interactions will be studied to determine their effect on the supramolecular structure of the compounds.

1.7 Objectives

The objectives of this study are:

1. To synthesize new cocrystals compounds of aminopyridine, aminopyrimidine and aminotriazine derivatives with a variety of carboxylic acids.

2. To characterize and analyze the formation of supramolecular assembly of the cocrystals.

3. To investigate the effect of hydrogen bond interaction by theoretical analysis.

4. To study the effect of the synthons on the supramolecular network of the compounds.

CHAPTER 2

LITERATURE REVIEW

In the crystal engineering, the design and synthesis of cocrystals have become a popular area of cocrystal research due to their versatility to exhibit the supramolecular synthons network. The synthons that formed between carboxylic acids and nitrogen heterocyclic rings is the most exploited synthons for designing cocrystal especially ring system forming a graph-set motif of $R_2^2(8)$ (Lynch & Jones, 2004). Carboxylic acid groups are very useful in molecular recognition (Arbuse *et al.*, 2007). They also possess tremendous ability in forming self assemblies and can easily bind with heterocyclic compounds (Lackinge *et al.*, 2009; Kathalikkattil *et al.*, 2011; Somphon *et al.*, 2013). Generally, in a cocrystal architecture, homosynthons and heterosynthons are formed depending on the molecular architecture and the positions and properties of functional groups. However, supramolecular heterosynthons (the substituted nitrogen heterocyclic system with carboxylic acids group) are statistically higher compared to the individual homosynthons (Allen *et al.*, 1998; Allen *et al.*, 1999).

The introduction of spectroscopic method has helped researchers to characterize, determine and understand the molecular and crystal structure of a cocrystal. Fourier Transform Infra-Red (FT-IR) spectroscopy, Nuclear Magnetic Resonance (NMR), Powder X-ray Diffraction (PXRD) and Single Crystal X-ray Crystallography are the most common methods being used for characterization and structural determination of cocrystals.

2.1 Nitrogen Heterocyclic Compound

Nitrogen heterocyclic compounds play an important role in the study of pharmaceuticals and agrochemicals. Many derivatives of nitrogen heterocyclic rings such as pyridine, pyrimidine and triazine derivatives have been synthesized in recent years. The schematic of the nitrogen heterocyclics are shown in Scheme 2.1.

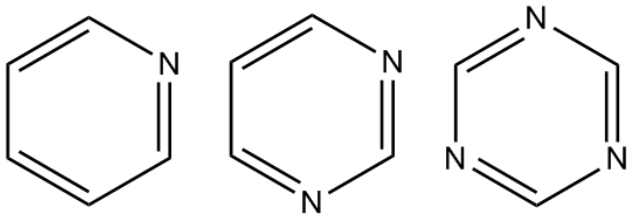

Pyridine (a) **Pyrimidine (b)** **Triazine (c)**

Scheme 2.1 The schematic of nitrogen heterocyclic such as pyridine, pyrimidine and triazine (Joule & Mills, 2010).

This study focuses specifically on the ability of carboxylic acids to form reliable and stable supramolecular heterosynthons with the aminopyridine, aminopyrimidine and aminotriazine derivatives to form cocrystals. The addition of an amino group to the former N-heterocylic gives a stronger balancing as a competitive binding site for carboxylic acids (Aakeröy *et al.*, 2006). The probabilities of formation of intermolecular hydrogen bonds between chemical groups containing at least one strong hydrogen bond donor group formed the most exploited supramolecular synthon in designing cocrystals (Shattock *et al.*, 2008).

Pyridine and its derivative, 2-aminopyridine is primarily used as an intermediate in the manufacturing of pharmaceuticals, particularly in anti-histamines and piroxicam. Lornoxicam and Tenoxicam are considered as new non-steroidal,

anti-inflammatory drugs of the oxicam class inhibiting cyclooxygenase, the key enzyme of prostaglandin biosynthesis at the site of inflammation (Baltork *et al*., 2008).

Pyrimidines and aminopyrimidine derivatives are biologically important compounds that manifest themselves in nature as components of nucleic acids. The functions of nucleic acids are explicitly determined by hydrogen-bonding patterns including base pairing, which is responsible for genetic information transfer. Their interactions with carboxylic acids are involved in protein−nucleic acid recognition and drug−protein recognition processes. Cocrystals of aminopyrimidine with carboxylic acids represent model systems where the hydrogen-bonded supramolecular motifs can be studied (Ebenezer & Muthiah, 2012).

Triazine derivatives have shown antitumor activity as well as broad range of biological activities like anti-angiogenesis and antimicrobial effects (Bork *et al*., 2003). The organic and inorganic complexes of triazine form well defined non-covalent supramolecular architectures *via* multiple hydrogen bonds constituting arrays of hydrogen-bonding sites (MacDonald & Whitesides, 1994).

2.2 Supramolecular Structure and Characterization of Cocrystal

From the best of our knowledge, there is no theoretical calculations have been reported so far for acid-base cocrystals consisted of 2-aminopyridine, 2-aminopyrimidine or 2-aminotriazine with various of carboxylic acid moieties. Therefore, the literature review in this thesis will discuss the supramolecular structure of cocrystals in the solid state condition.

Lemmerer *et al*. (2015) have studied cocrystals and salts to analyze the pKa values for the formation of the crystals. They have studied 2-chloro-4-nitrobenzoic acid donor with different substituents of pyridine acceptor which formed cocrystals and salts. Figure 2.1 shows the molecular structure of the cocrystals and salts with their ΔpKa values. The supramolecular heterosynthon COO—H···$N_{pyridine}$ formed between a carboxylic acid donor and a pyridine acceptor is observed in all the cocrystals. In the molecular salt structures, proton transfer has occurred to the pyridinium base to form a COO^{-}···H—$N_{pyridine}^{+}$ hydrogen bond. They found out that the ΔpKa values above 3 formed molecular salts and values below zero formed cocrystals. However, in intermediate range, there is a possibility of salts or cocrystals formation.

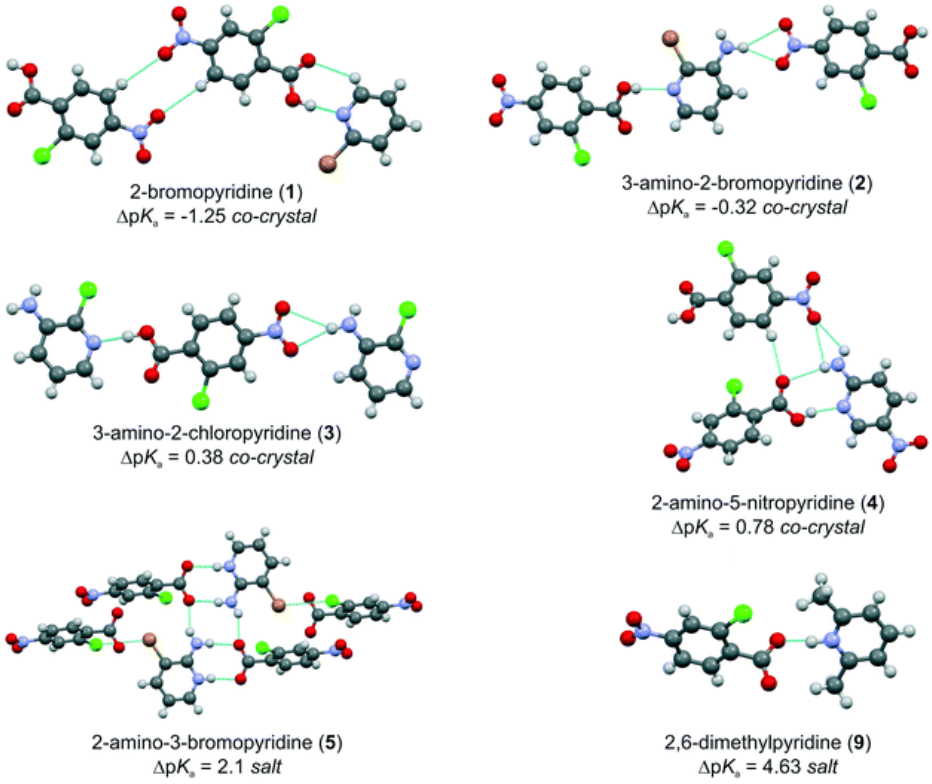

Figure 2.1 Examples of cocrystals and salts (Lemmerer *et al*., 2015).

The cocrystal structure of 2-amino-5-chloropyridine benzoic acid studied by Hemamalini and Fun (2010a) (Figure 2.2b) shows that 2-amino-5-chloropyridine molecules interact with the carboxyl group of benzoic acid molecules through N—H···O and O—H···N hydrogen bonds to form a cyclic hydrogen-bonded motif $R_2^2(8)$ (Bernstein *et al.*, 1995). The C—O bond lengths for the carboxylic acid of the benzoic acid are 1.3190 (15) Å for O–C and 1.2250 (15) Å for O=C, thus, no proton transfer from the carboxyl group of benzoic acid. The molecules are linked into chains parallel to the [001] direction (Figure 2.2b). The neighbouring 2-amino-5-chloropyridine molecules are centrosymmetrically paired through C—H···Cl hydrogen bonds, forming another $R_2^2(8)$ motif and are further stabilized by weak C—H···O hydrogen bonds.

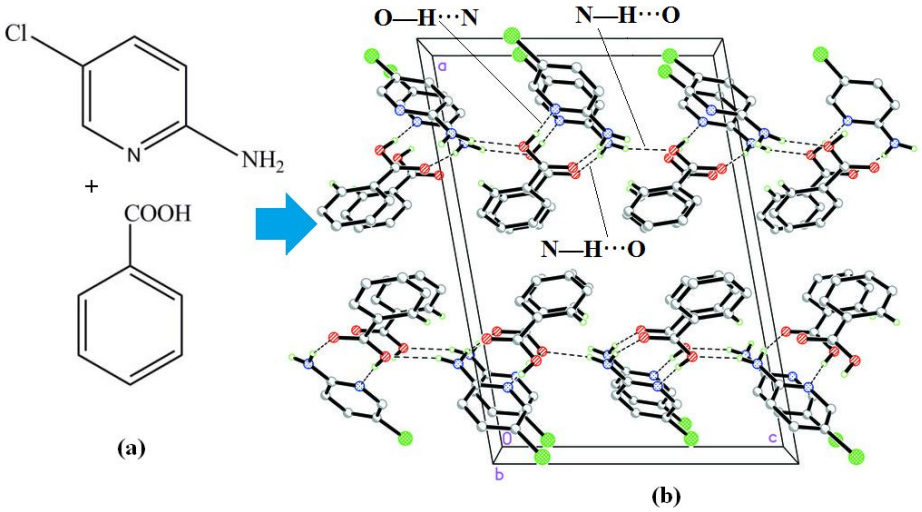

Figure 2.2 (a) Scheme and (b) the crystal packing of the molecular structure of 2-amino-5-chloropyridine benzoic acid (Hemamalini & Fun, 2010a).

The formation of $R_2^2(8)$ ring motif is also reported by Hemamalini and Fun (2010b) in the cocrystal structure of 2-amino-5-bromopyridine benzoic acid where the $N_{pyridine}$ molecule interact with the carboxylic group of the respective benzoic acid molecules through N—H···O and O—H···N hydrogen bonds as shown in

Figure 2.3. This cocrystal structure also shows that no proton transfers from the carboxyl group of benzoic acid since the C–O bond lengths for the carboxylic acid of the benzoic acid are 1.317 (2) Å for O—C and 1.225 (2) Å for O=C.

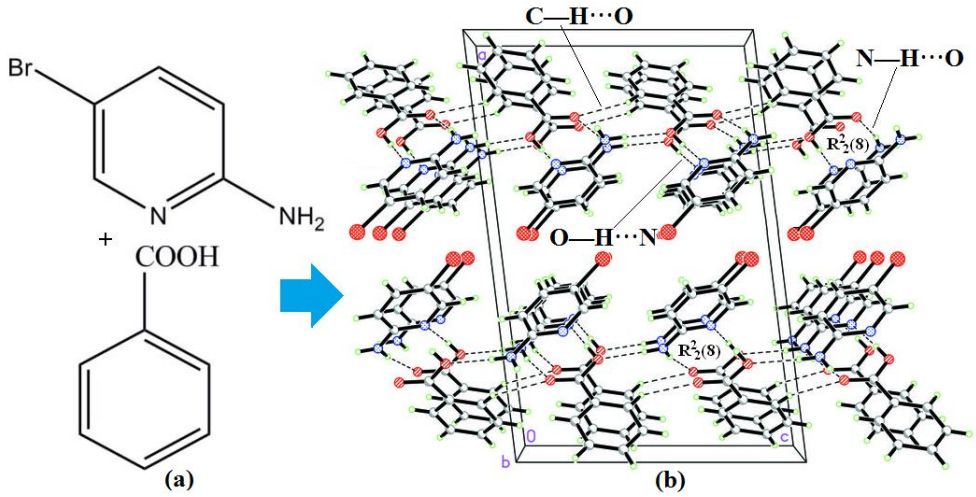

Figure 2.3 (a) Scheme and (b) the crystal packing of the molecular structure of 2-amino-5-bromopyridine benzoic acid (Hemamalini & Fun, 2010b).

In the crystal packing (Figure 2.3b), the $R_2^2(8)$ ring motif are linked into 2-dimensional networks parallel to the (100) plane by strong N—H···O and weak C—H···O interactions.

Thanigaimani *et al.* (2006) reported an array of six hydrogen bonds forming ring motifs of $R_2^3(6)$, $R_2^2(8)$, $R_2^4(8)$, $R_2^2(8)$ and $R_2^3(6)$ (Figure 2.4a) within the 2-amino-4, 6-dimethoxypyrimidine 4-aminobenzoic acid crystal structure.

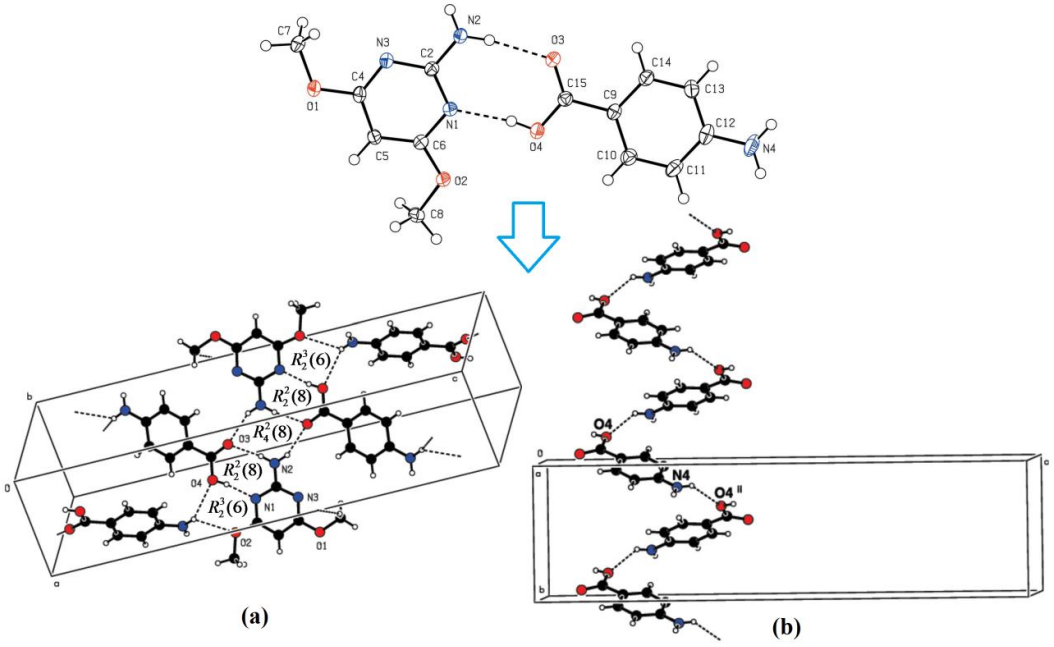

Figure 2.4 Molecular structure of 2-amino-4,6-dimethoxypyrimidine 4-aminobenzoic acid: (a) Hydrogen bond pattern and (b) hydrogen pattern in supramolecular chain along the *c*-axis (Thanigaimani *et al.*, 2006).

The generation of homosynthon and heterosynthon through hydrogen interactions was reported by Hemamalini *et al*. (2014). In their report, 2-amino-6-chloropyridine in neutral form can be self-assembled through N—H···N hydrogen bonds to form $R_2^2(8)$ ring motif homosynthon (Figure 2.5). These dimers are further interconnected by another N—H···N and C—H···Cl hydrogen bonds, forming sheets parallel to the *bc* plane as shown in Figure 2.5.

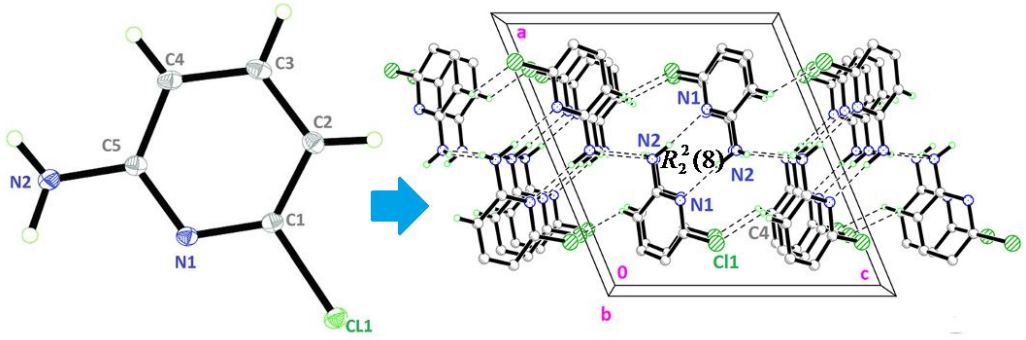

Figure 2.5 Hydrogen pattern in 2-amino-6-chloropyridine represent homosynthon (Hemamalini *et al*., 2014).

This ligand can also form $R_2^2(8)$ ring motif heterosynthon by interacting with carboxylic acid molecules through N—H···O and O—H···N hydrogen bonds (Figure 2.6a). Intermolecular N—H···O (1/2+*x*,3/2–*y*,2–*z*) hydrogen bonds link the heterosynthons into zig-zag chains as illustrated in Figure 2.6(b).

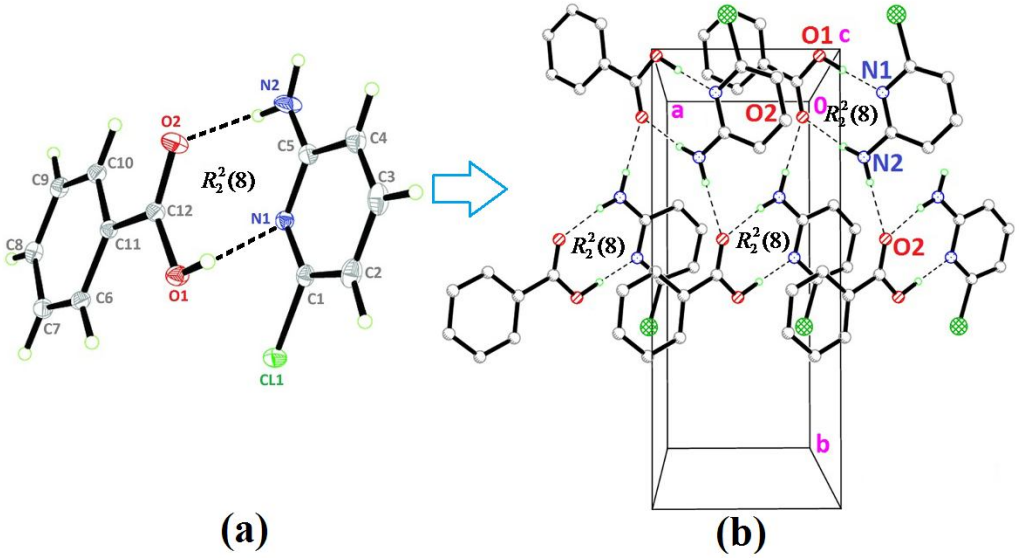

Figure 2.6 Hydrogen pattern in 2-amino-6-chloropyridine benzoic acid represent (a) $R_2^2(8)$ ring motif heterosynthon; (b) supramolecular zig-zag chains (Hemamalini *et al.*, 2014).

Hemamalini *et al.* (2014) also reported the existence of non-covalent interactions has forming arrays of donor (D) and acceptor (A) atoms within the crystal structure. In 2-amino-6-chloropyridine 3-chlorobenzoic acid, the heterosynthons are centrosymmetrically paired via N—H···O hydrogen bonds, forming a complementary DADA [D = donor and A = acceptor] array of quadruple hydrogen bonds. The DADA array of hydrogen bonding motif is represented by graph-set notations of $R_2^2(8)$, $R_4^2(8)$ and $R_2^2(8)$ in sequence as shown in Figures 2.7.

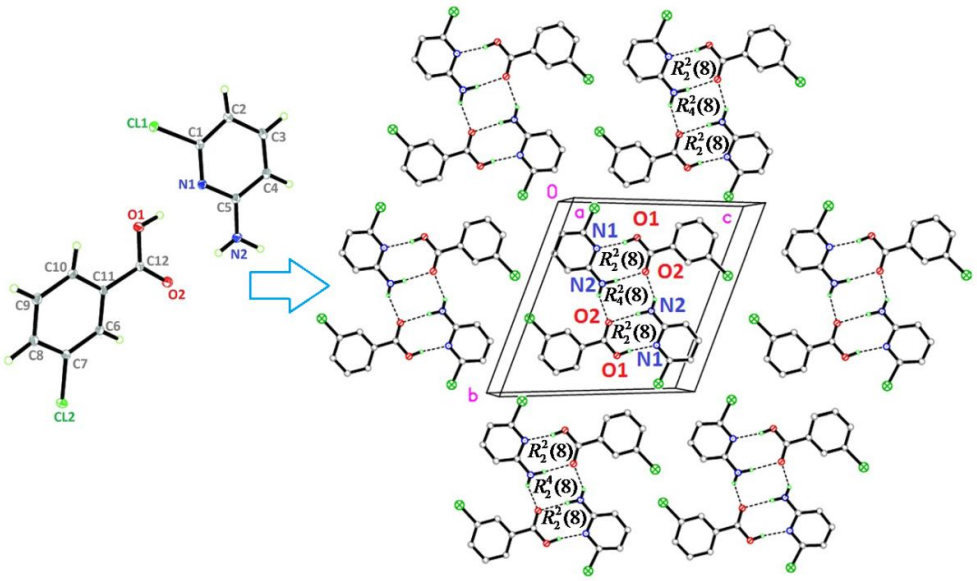

Figure 2.7 View of the complementary DADA arrays of quadruple hydrogen pattern in 2-amino-6-chloropyridine 3-chloropyridine (Hemamalini *et al.*, 2014).

Ebenezer and Muthiah (2012) were investigating aminopyrimidine derivatives with carboxylic acid through recurrently occurring synthons. In their report on 2-amino-4, 6-dimethoxypyrimidine 2-chlorobenzoic acid cocrystal, the main motif $R_2^2(8)$ is assembled through a complimentary hydrogen bond interactions between the carboxylic acid and the amino-pyrimidine moiety to form a dimeric unit. In the crystal structure of the cocrystal, these dimeric units are connected by N—H···O (2–*x*,–*y*,1–*z*) hydrogen bonds forming linear heterotetrameric synthons (Figure 2.8). These tetramers are planar and are interconnected into infinite 1-D tape *via* two symmetry related hydrogen bonds involving O atoms of symmetry related methoxy group of neighbouring pyrimidine rings forming a homosynthon with graph set notation $R_2^2(6)$.

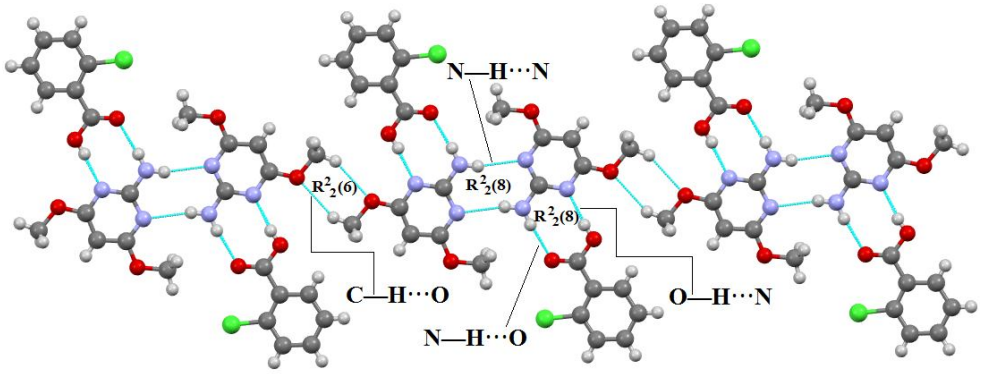

Figure 2.8 View of heterotetramer infinite tape connected by $R_2^2(6)$ synthon (Ebenezer & Muthiah, 2012).

The neighbouring tapes are interconnected through weak C—H···O intermolecular hydrogen bonds involving the acid rings and one of the methoxy groups attached to the pyrimidine rings to form a supramolecular sheet (Figure 2.9).

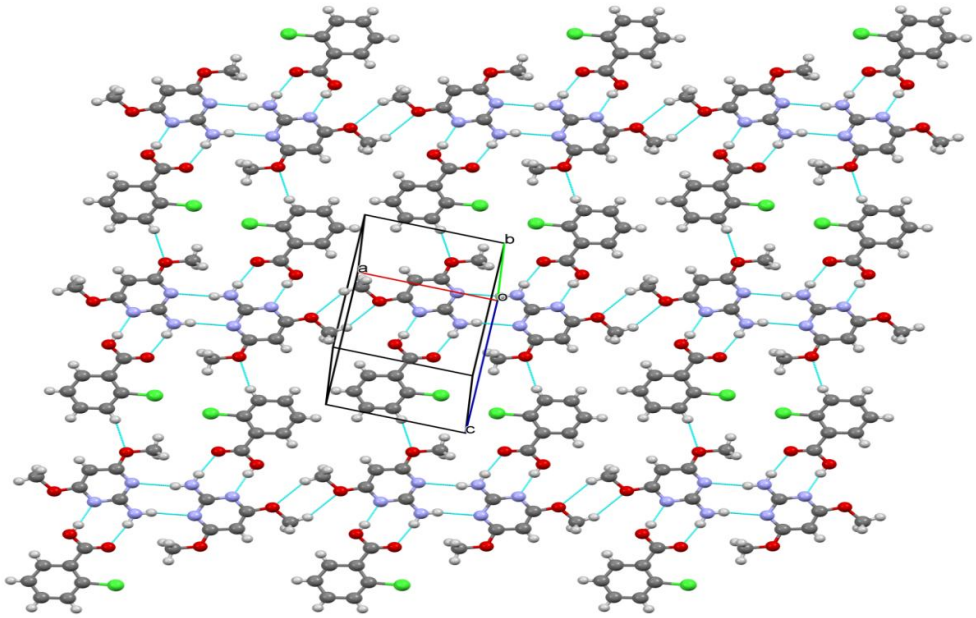

Figure 2.9 Supramolecular sheet formed by interconnection of tape along (122) plane (Ebenezer & Muthiah, 2012).

Ebenezer and Muthiah (2012) also reported the primary $R_2^2(8)$ synthon found in 2-amino-4, 6-dimethoxypyrimidine 3-methylbenzoic acid where the hydrogen bonds (O—H···N, N—H···O and N—H···N) involving the amino and hydroxyl

protons of carboxylic acid as donors and the two pyrimidine nitrogens including the oxygen of the carbonyl group as acceptors formed a linear heterotetrameric synthon. These tetramers are connected *via* $R_2^2(6)$ synthon generated from symmetry related C—H···O intermolecular hydrogen bonds and assembled into infinite 1-D tapes (Figure 2.10).

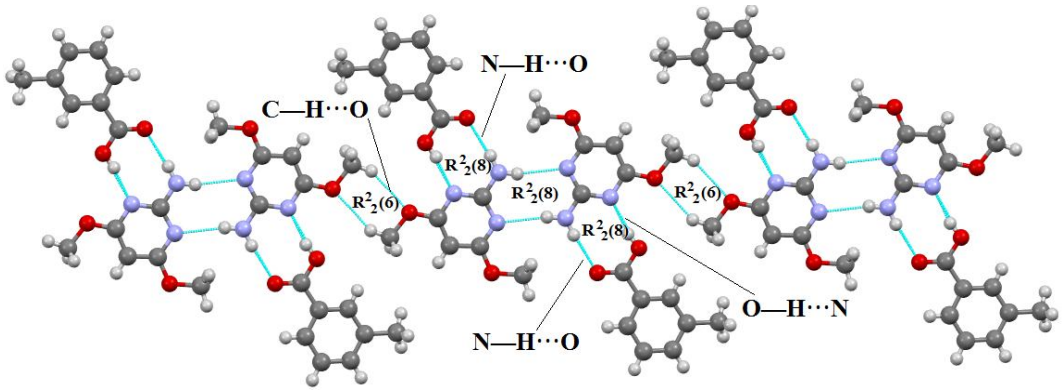

Figure 2.10 View of extension infinite tape connected by $R_2^2(6)$ synthon (Ebenezer & Muthiah, 2012).

Interactions between aminotriazine and the carboxyl group of sorbic acid molecules *via* N—H···O and O—H···N hydrogen bonds form a supramolecular heterosynthon with graph set notation $R_2^2(8)$ (Thanigaimani *et al*., 2007). In the crystal packing, the triazine molecules are base-paired with a graph set of $R_2^2(8)$ on either side *via* N—H···N hydrogen bonds, forming a supramolecular ribbon along the *c*-axis (Figure 2.11). These supramolecular ribbons are interlinked by N—H···O hydrogen bonds involving the 2-amino group of the triazine molecules and the carboxyl O atom of the sorbic acid molecules.

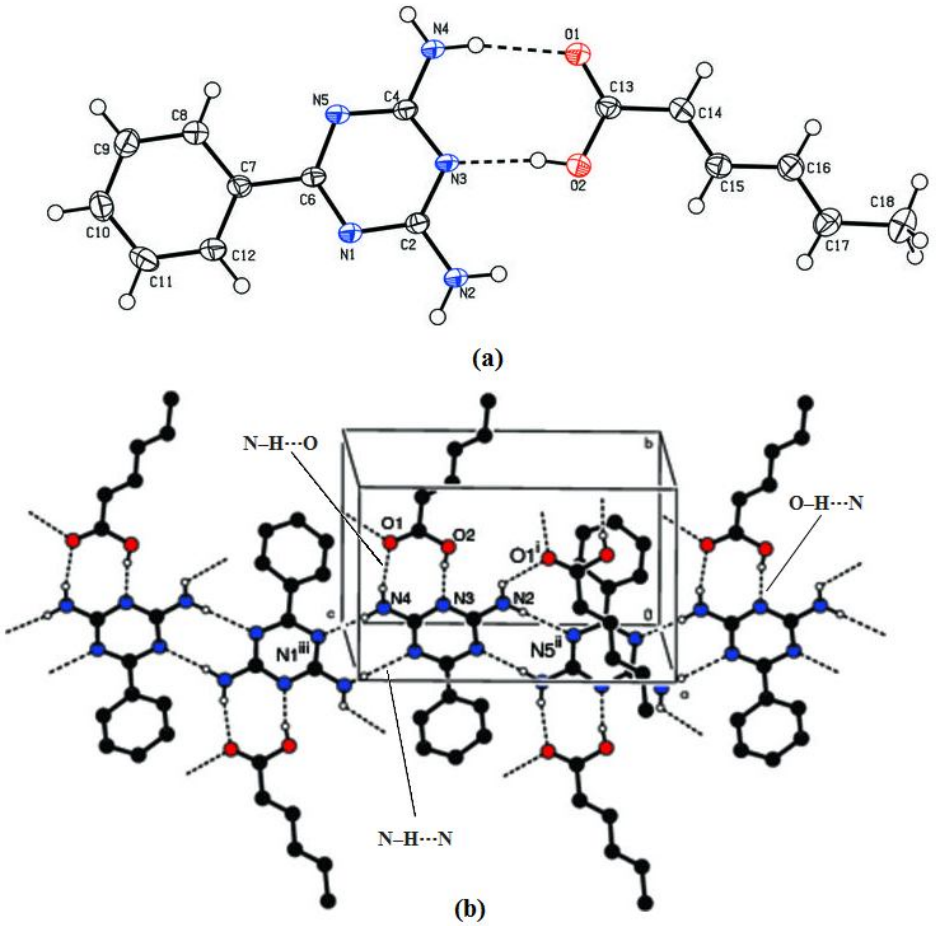

Figure 2.11 (a) The asymmetric unit and (b) the crystal packing of 2,4-diamino-6-phenyl-1,3,5-triazine–sorbic acid (1/1) showing 50% probability displacement ellipsoids. Dashed lines indicate hydrogen bonds [symmetry code: (i) *x*, −*y*+1, *z*−1/2; (ii) *x*, −*y*, *z*−1/2; (iii) *x*, −*y*, *z*+1/2] (Thanigaimani *et al*., 2007).

Amit *et al*. (2013) studied the influence of shape of conformers on supramolecular assemblies of molecular adducts of 2, 4-diamino-6-phenyl- 1, 3, 5-triazine with conformers of different shape. They concluded that the linear ligands formed 8-membered cyclic network while bend ligands preferred to form 6-membered tapes (Figure 2.12).

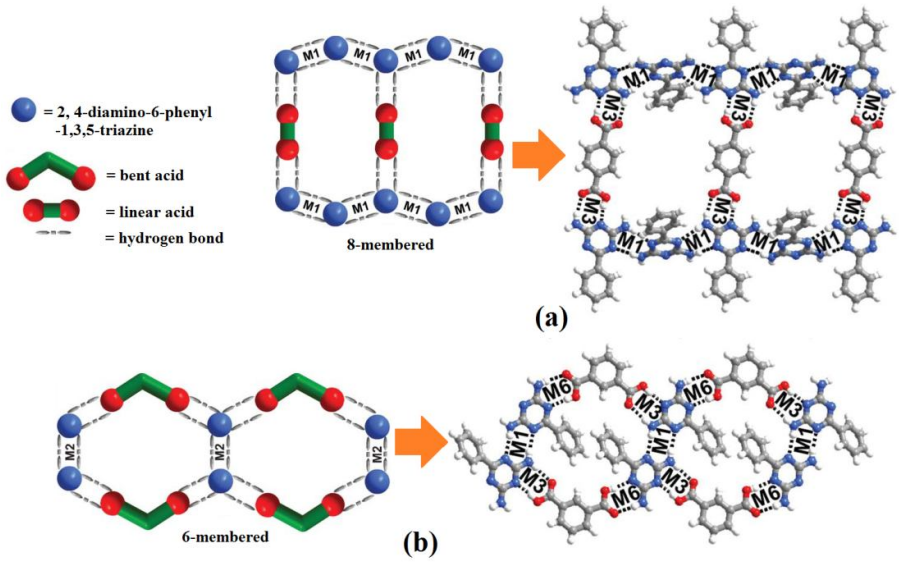

Figure 2.12 (a) Linear acid formed 8-membered cyclic tape network; (b) Bent acid formed 6-membered cyclic tape network (Amit *et al.*, 2013).

The ability of carboxylic acids to form self assemblies was discussed by Jali and Baruah (2013). They reported on the cisoid and transoid geometry of the carboxylic acids in cocrystals of 2, 4-diamino-6-phenyl- 1, 3, 5-triazine and how these geometries influence the supramolecular of the cocrystals (Figure 2.13).

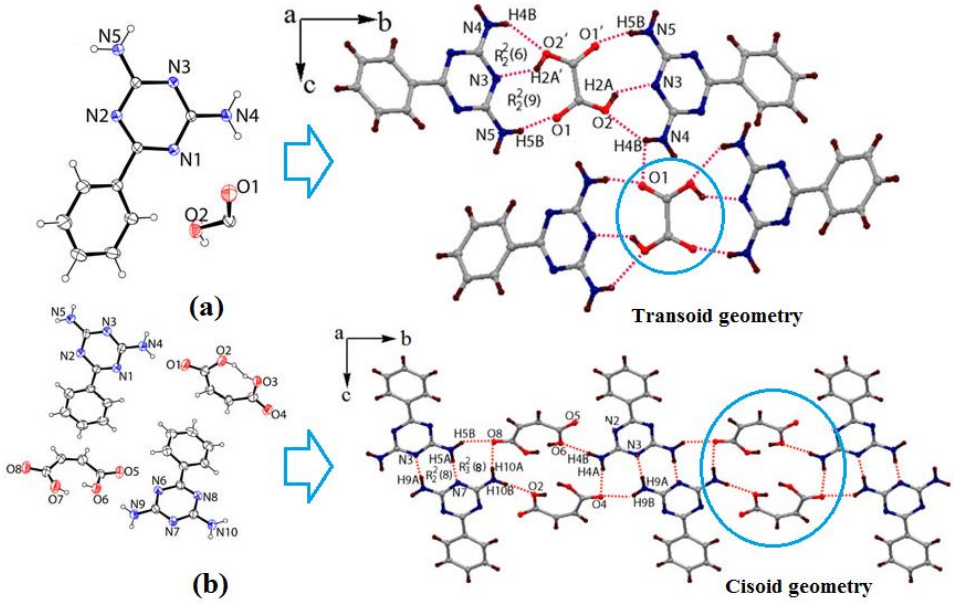

Figure 2.13 (a) The transoid geometry and (b) the cisoid geometry of the carboxylic acids in cocrystals of 2, 4-diamino-6-phenyl- 1, 3, 5-triazine (Jali & Baruah, 2013).